DESY 97-123E

April 1997

hep-ph/9706338 12 Jun 1997

The Standard Model Higgs: Discovery Potentials and Branching Fraction Measurements at the NLC

M. Sachwitz, H. J. Schreiber and S. Shichanin*

DESY-Institut für Hochenergiephysik, Zeuthen, FRG

* On leave of absence from Institute for High Energy Physics, Protvino, Russia

Abstract

We discuss discovery potentials for a 140 GeV Standard Model Higgs boson produced in e^+e^- collisions at 360 GeV, including all potential irreducible and reducible background contributions. In the second part of the study, we estimate the uncertainties expected for the branching fractions of the Higgs into $b\bar{b}$, $\tau^+\tau^-$, $\mathrm{WW}^{(*)}$ and into $c\bar{c} + gg$ including a realistic error estimation of the inclusive bremsstrahlung Higgs production cross section.

1 Introduction

The fundamental particles in the Standard Model (SM) [1], the gauge bosons, the leptons and quarks, acquire their mass by means of the Higgs mechanism [2]. This mechanism implies the existence of a real physical particle, the Higgs boson, and its discovery is the most important experiment for the standard formulation of the electroweak interactions.

However, in the SM the mass of the Higgs particle is unknown. A lower bound on the Higgs mass of about $M_H \geq 66$ GeV has been established so far from LEP I [3]; this limit can be raised to ~ 95 GeV in the second phase of LEP with a total energy of $\sqrt{s} = 192$ GeV [4]. Beyond the LEP II range, the multi-TeV pp collider LHC can cover the entire Higgs mass range up to the SM limit of about 800 GeV [5]. For M_H above ~ 150 GeV, the lepton channel $H^0 \longrightarrow 4l^{\pm}$ will provide a nearly background free signature, while below that value the rare photon decay $H^0 \longrightarrow \gamma\gamma$ is the sole decay channel, established so far. Due to the overwhelming QCD background, other H^0 decay modes cannot be explored or are difficult to detect. In the SM, the intermediate mass range from ~ 110 GeV, derived from the requirement of vacuum stability for a ~ 180 GeV top quark mass, to 180-200 GeV is a very attractive region for the Higgs mass.

Future e^+e^- linear colliders operating in the 300 to 500 GeV center-of-mass energy range, generically denoted as NLC (for Next Linear Collider) in the following, are the ideal machines to investigate the Higgs sector in this mass range since it can be easily discovered and all major decay modes can be explored. The search for the Higgs boson and the study of its properties are therefore of primary importance in the physics program at the NLC.

In order to access the actual capability of such a collider concept it is extremely interesting and appealing to apply recently developed tools, thanks to the effort of several groups, to an analysis of SM Higgs boson physics. In this study we include

- the full matrix elements for 4-fermion final states beyond the usual approximation of computing production cross sections of the Higgs and the Z boson times branching fractions into decay products;
- Higgs decay channels with SM decay fractions larger than $\sim$1% treated in a unified way;
- initial state QED and beamstrahlung;
- a detector response, with parameters of the detector as designed in a series of workshops for the e^+e^- linear collider Conceptual Design Report;
- all important reducible background expected to contribute.

In sects.2 and 3 we present some introduction to linear collider and detector aspects relevant for Higgs studies. Sect. 4 is devoted to a description of the event generation procedures. We then describe our analysis for the particular case of a cm energy $\sqrt{s} = 360$ GeV and a Higgs mass $M_H = 140$ GeV. It is shown that the Higgs can be observed with limited integrated luminosity and the inclusive Higgs cross section can be determined with high accuracy, without assumptions on the Higgs decay modes. Once the Higgs is found it is of great importance to measure the (relative) Higgs couplings to gauge bosons and fermions. We demonstrate the precision with which the branching fractions can be (easily) measured, allowing a potential discrimination of the SM Higgs from e.g. the lightest CP-even MSSM Higgs over a large range in $\tan\beta$. We are particularly concerned with simulations of both the signal and background rates for all important reactions expected to contribute at 360 GeV. The cm energy is chosen such that $t\bar{t}$ pair production as background is excluded by definition.

2 The center-of-mass energy spectrum and luminosity

The extremely high density to which the beam particles must be focused to produce sufficient luminosity for particle physics at a NLC results in a significant interaction rate between the particles of one beam and the collective electromagnetic fields produced by the particles in the opposite beam. A major consequence of this is that the cm energy spectrum at which e^+e^- interaction takes place is not at all monochromatic. Radiation of photons during the beam-beam collision, the so called beamstrahlung, will result in a $\sqrt{s}$-spectrum that depends in detail on the energy and bunch characteristics of each beam. In our study we have used, as an example, the beam parameters for the TESLA design [6], which are in many respects typical of most machine designs studied so far. In particular,

the beamstrahlung simulation used in this study includes the effects of multiple radiation and beam-beam disruption [7].

Besides beamstrahlung, a further reduction of the initial state energy occurs due to radiation of photons off the beam particles (ISR). In our simulation, ISR has been included as suggested in [8] and convoluted with the beamstrahlung spectrum. The net result of both effects on the cm energy distribution can be seen in Fig.1 for a few reactions relevant to Higgs studies.

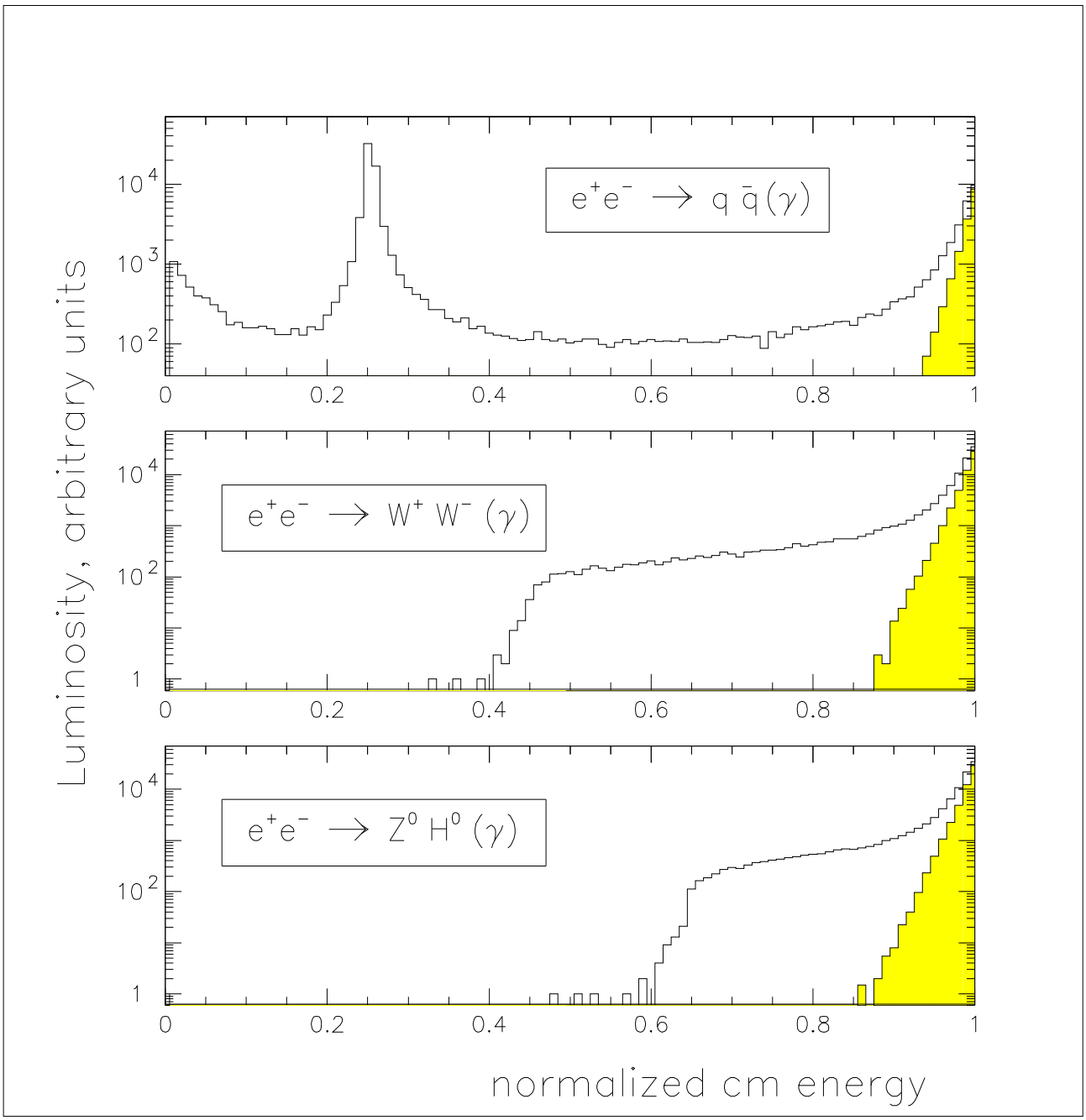

Figure 1: *Luminosity spectra expected after convolution with initial state radiation (ISR) and beamstrahlung for various reactions. The shaded histograms show the energy degradation due to the beamstrahlung only. The nominal cm energy is 360 GeV.*

Here, the hatched histograms reveal the effect from beamstrahlung alone, for the TESLA design. In contrast to ISR effects, beamstrahlung energy degradation is, as expected, reaction-independent. If the cm energy cannot be degraded by photon radiation to the Z^o pole, such as in ZH or WW production, beamstrahlung contributes typically one-third of the total energy loss during beam-beam collision. Beam energy spread expected to be $\sim 0.1\%$ has been neglected.

In this study, all event rates have been computed by convoluting the luminosity spectrum with the relevant cross section evaluated at the reduced cm energy. Thus, event rates of reactions with an 1/s-cross section dependence are somewhat enhanced while those with a logarithmic cross section s-dependence are only little affected by beamstrahlung and ISR. Since most of our signal and background rates possesses some sensitivity to the details of the cm energy distribution, we varied this spectrum within reasonable ranges and found that the conclusions we draw are not altered.

The luminosity is assumed to be $5 \cdot 10^{33}\mathrm{cm}^{-2}\mathrm{sec}^{-1}$ [6], so that for two years of running (with 10^7 sec per annum) an accumulated luminosity of 100 fb^{-1} should be obtained.

3 Detector response

The properties of a detector that are necessary to successfully carry out analyses of the Higgs boson physics at the NLC have been developed in the course of the 'Conceptual Design for an e^+e^- Linear Collider and Detector' of the European high-energy physics community [6]. The basic components of the detector are a vertex detector, a tracker, an electromagnetic and a hadronic calorimeter, a muon detector and a luminosity counter. The parameters of the detector components (resolutions, acceptances and granularities) relevant for this study are summarized in Table 1. As can be seen, for the detector properties we assume no extension of any technology beyond what exists or is feasible in the near future, although we can anticipate that improvements in the techniques and technologies used in design and construction of detector components will occur. In this analysis the emphasis is addressed to the tracker, the vertex detector and the calorimeters.

The detector response is obtained by modifying the generated particle momenta, energies, directions and nature in the following manner. At first, particles within the acceptance regions are divided into isolated particles and energetic clusters. Particles are called isolated if they have a 'large' distance to any other when entering the electromagnetic calorimeter, otherwise they are combined to clusters. The isolation criteria are based on the cell size of the calorimeters.

Vertexing	$\sigma_{imp}(R\phi) = 10\ \mu m \oplus 30\mu m\ /psin^{3/2}\Theta$ $\lvert cos\Theta\rvert = 0.95$
Tracking	$\sigma_{p_\perp}/p_\perp = 1.5 \cdot 10^{-4}\ p_\perp(GeV) \oplus 0.01$ $\lvert cos\Theta\rvert \leq 0.95$ radius: 1.5 m length: 5.0 m
Electromagnet Calorimeter	$\sigma_E/E = 0.10\ /\ \sqrt{E(GeV)} \oplus 0.01$ cell size: $0.7^o \times 0.7^o$ $\lvert cos\Theta\rvert \leq 0.98481\ \ (\hat{=} 10^o ... 170^o)$
Hadronic calorimeter	$\sigma_E/E = 0.50\ /\ \sqrt{E(GeV)} \oplus 0.04$ cell size: $2^o \times 2^o$ $\lvert cos\Theta\rvert \leq 0.98481\ \ (\hat{=} 10^o ... 170^o)$
Muon detector	Fe yoke instrumented as tail catcher and muon tracker
Luminosity counter	$\sigma_E/E = 0.12\ /\ \sqrt{E(GeV)} \oplus 0.02$ cell size: $2^o \times 2^o$ $4^o < \Theta < 8^o; \qquad 172^o < \Theta < 176^o$

Table 1: *Detector parameters. The symbol $\oplus$ means quadratic sum.*

For clusters, the electromagnetic and hadronic energy components undergo separate smearing by a Gaussian according to the parameters of Table 1 and are then combined to the total cluster energy. Their directions are also Gaussian-

modified according to the granularities. Note that for charged isolated particles, the smeared momentum from the tracker is used except in the case when a better energy value from the calorimeter exists. We apply for the transverse momentum smearing the formula

$$\frac{\sigma_{p_\perp}}{p_\perp} = Ap_\perp \oplus 1\%$$

with A $= 7 \cdot 10^{-5}$. This resolution parameter is expected from the combined vertex detector and the central tracker together with a constraint from the main e^+e^- vertex. The tracker resolution scaling inversely proportional with the square of the projected track length is accounted for in the program. Azimuthal and polar angles of charged particles are smeared with standard deviations of 1 mrad and 2 mrad, respectively. Isolated neutral hadrons (photons) are modified according to the resolution parameters of the hadron (electromagnetic) calorimeter. Charged particles are required to have a minimum transverse momentum of 200 MeV, while an electromagnetic (hadronic) calorimeter entry should have at least a deposited energy of 100 (300) MeV; otherwise they are removed. Electrons (muons) are misinterpreted as charged pions with 1% (2%) probability, and muons should exceed an energy of 3 GeV. A solenoidal magnetic field of 3 Tesla is assumed.

The relatively long lifetime of the b-quark, expected preferentially to be produced from Higgs boson decays, gives rise to decay vertices displaced from the primary e^+e^- vertex or, equivalently, to tracks with large impact parameters. We included these decays by simulating the performance of a vertex detector and making use of the impact parameter information in the plane perpendicular to the beam direction. For each track projection we compute its distance of closest approach to the primary vertex, b, and assume that the measurement error on b can be parameterized as

$$\sigma_b = \sqrt{A^2 + [B/(p \sin^{3/2}\Theta)]^2}\,,$$

where the parameters A $= 10$ μm and B $= 30$ μm reflect the intrinsic resolution of the vertex detector and the effect of multiple scattering of particles traversing the beam pipe and the detector. A charged particle is defined to be a 'high impact parameter track' if it is within the vertex detector acceptance region and has a value of $\mathrm{b}_{norm} = \mathrm{b}/\sigma_b$ greater than two (or three). An upper limit of the impact parameter has also been introduced to suppress contamination from K_S and Λ decays. Our vertex detector simulation is kept simple and generic so that the success of the analysis does not depend on specific details of the device. As soon as a detailed design of the vertex detector exists, dedicated Monte Carlo simulations will be mandatory.

4 Event generation

We have assumed that the Standard Model with three generations of quarks and leptons is a correct description of nature and the Higgs particle couples to bosons and fermions as predicted by the SM model.

The reactions considered in this note are listed in Table 2.

For the 2-to-4 body reactions (1) - (5), the full matrix elements are used for event generation, beyond the usual approximation of computing production cross sections times branching fractions. In this way, contributions of non-leading diagrams, interferences, correct spin structures and non-zero fermion masses are taken into account. The calculation consists of two main steps. The generation of Feynman diagrams, the analytical expressions for the matrix elements squared and the corresponding optimized Fortran code have been obtained by means of the computer package CompHEP [9]. The integration over phase space and the generation of the event flow have been done with the help of the adaptive Monte Carlo package BASES/SPRING [10]. It is worthwhile to point out that because of the complicated phase space structure of 4-fermion final states and the occurrence of singularities, an appropriate choice of variables and smoothing of singularities were mandatory. Today's version of CompHEP offers all features needed to overcome these problems.

So far, the reaction $e^+e^- \to \mu^+\mu^- b\bar{b}$ has been studied in e.g. [11]. It has been found that this reaction has the cleanest signature for the Higgs but the event rate is rather small. At least six times more Higgs events are expected in the reaction $e^+e^- \longrightarrow \nu\bar{\nu}\; b\,\bar{b}$, for which complete tree-level calculations can be found in [12]. Here, some extra contribution comes from the fusion process $e^+e^- \longrightarrow \nu\bar{\nu}\; H^0$. The reaction $e^+e^- \to e^+e^- b\bar{b}$ turned out to be the most complicated one from the calculational point of view [13], and the extraction of the Higgs out of a background two orders of magnitude larger requires well designed cuts. Higgs production and its detection potential have also been considered in the reaction $e^+e^- \to b\bar{b}$ + 2 jets [14].

These studies restricted to b-quarks in the final state have now been extended to include the quark states u, d, s, c and b. In addition, reaction (3), $e^+e^- \to \tau^+\tau^- q\bar{q}$, is included in the analysis. Its tree-level calculation is performed in analogy with that of reaction (1), $e^+e^- \to \mu^+\mu^- q\bar{q}$, with the substitution $m_\mu \to m_\tau$ and the restrictions to $Z^0 \to q\bar{q}$ and $H^0 \to \tau^+\tau^-$ decays.

In order to avoid unnecessary large event samples the following conditions were applied during event generation:

- for reactions (1)-(3): M($q\,\bar{q}$)> 50 GeV, $|\cos\,\Theta\;(q,\bar{q})| < 0.993$ and M($l\bar{l}$) > 30 GeV;

Reaction		cross section, fb	signal cross section, fb	comments
$e^+e^- \to \mu^+\mu^- q\bar{q}$	(1)	50.0	2.85	see text
$e^+e^- \to e^+e^- q\bar{q}$	(2)	4450	4.62	see text
$e^+e^- \to \tau^+\tau^- q\bar{q}$	(3)	51.9	2.96	$H^0 \to \tau^+\tau^-$ and $Z^0 \to q\bar{q}$ only
$e^+e^- \to \nu\bar{\nu} q\bar{q}$	(4)	347	33.0	see text
$e^+e^- \to 2q2\bar{q}$	(5)	434	55.6	see text
$e^+e^- \to W^+W^-$	(6)	11200	-	
$e^+e^- \to e\nu W$	(7)	3650	-	WW excluded
$e^+e^- \to q\bar{q}(\gamma)$	(8)	33900	-	
$e^+e^- \to HZ$ $\to WW^*Z$ $\to 3q3\bar{q}$	(9)	-	18.5	
$e^+e^- \to WWZ$ $\to 3q3\bar{q}$	(10)	4.21	-	
$e^+e^- \to ZZZ$ $\to 3q3\bar{q}$	(11)	0.31	-	
$e^+e^- \to t\bar{t}$	(12)	-	-	
$e^+e^- \to \nu\bar{\nu} gg$	(13)	-	2.36	
$e^+e^- \to q\bar{q}gg$	(14)	-	4.20	

Table 2: *Reactions involved in this study and their total and signal cross sections at $\sqrt{s} = 360$ GeV and $M_H = 140$ GeV. ISR and beamstrahlung are included. We assume a top mass being somewhat above 180 GeV.*

- for reaction (4): either M($q\,\bar{q}$)$>$ 50 GeV and $|\cos\,\Theta\ (q,\bar{q})| < 0.993$ or M($q\,\bar{q}$)$>$ 100 GeV and $|\cos\,\Theta\ (e^+)| < 0.9962$ and $|\cos\,\Theta\ (e^-)| < 0.9962$;
- for reaction (5): M($q\,\bar{q}$)$>$ 10 GeV, $|\cos\,\Theta(q,\bar{q})| < 0.993$, $|\cos\,\Theta(q)| < 0.993$ and $|\cos\,\Theta(\bar{q})| < 0.993$.

At cm energies 300-500 GeV, high p_t-background contributions are theoretically well understood and accurately calculable. Most of the background expected is due to hard electroweak and QCD processes. They are also listed in Table 2, together with their cross sections. As can be seen, these reactions contribute more than 4 million events to the data volume for an integrated luminosity of 100 fb^{-1}. Such an enormous data sample might obscure and/or mimic a Higgs signal. Hence, we include these channels in our simulation procedures at the same level as the signal reactions in order to make a signal-to-background analysis as meaningful as possible.

A Higgs boson with a mass of 140 GeV decays in almost 50 % of the cases into WW^*. The knowledge of this branching fraction is of importance because it helps greatly to establish the nature of the Higgs and, together with the cross section of the WW-fusion reaction, to determine the total width of the Higgs. In order to ensure large statistics for the $H^0 \longrightarrow$ WW* decay, the $W \to q\bar{q}$ and $Z \to q\bar{q}$ decays are considered in this paper. It would be desirable to embed the signal channel $e^+e^- \longrightarrow Z^0\,H^0 \longrightarrow (q\,\bar{q}\ )$(WW*) in a general 2-to-6 body event generator, so that besides the signal irreducible background and interferences could be also addressed. Such an event generator is at present not available. Therefore, the signal channel has been processed in the usual approximation of computing production cross sections times the $H^0 \longrightarrow$ WW* branching fraction, as indicated in Table 2. The SM 6-jet processes, $e^+e^- \to WWZ$ and ZZZ, are expected to be the only significant sources of background; they were generated in the same manner as the Higgs channel, with cross sections as listed in Table 2.

The $H^0 \longrightarrow c\,\bar{c}\ +$ gg decay occurs in a few percent of the cases. We try to isolate this decay mode using the 2-jet missing energy and the 4-jet reactions (4), (5), (13) and (14). We would like to point out that reaction (13) is free of tree-level background, whereas the $q\,\bar{q}$ gg background is already accounted for by gluon radiation in reaction (8).

Reactions (6), (8), (13) and (14) have been generated by means of the package PYTHIA 5.7 [15] including the beamstrahlung effects [16], while for reactions (7) and (9)-(11) CompHEP has been used. For all reactions considered, the JETSET 7.4 package [15] has been used for quark and gluon fragmentation

and unstable particle decays. The events generated are fed into a fast detector simulation program as described in sect. 3.

One should emphasize that, to a good approximation, dedicated calculations of the electroweak part of the reactions considered have achieved very high accuracy but that relatively large uncertainties exist in the perturbative parton shower or non-perturbative hadronization procedures. This rises the question of the reliability of such calculations for the study of hadronic and mixed hadronic-lepton final states. In this paper we adopted a pragmatic solution: we used a standard interface program for parton-shower and hadronization procedures and rely on its usefulness for our application.

5 Higgs Discovery Potential

Basically, the Higgs can be produced by the bremsstrahlung process[17]

$$e^+e^- \longrightarrow Z^* \longrightarrow Z^0 H^0 \tag{15}$$

or by the fusion of WW and ZZ bosons[18]

$$e^+e^- \longrightarrow \nu\overline{\nu}H^0 \tag{16}$$

$$e^+e^- \longrightarrow e^+e^-H^0\,. \tag{17}$$

At $\sqrt{s} = 360$ GeV and $M_H = 140$ GeV, the bremsstrahlung process is about four times more important than the fusion reactions. This is in good approximation also true if ISR and beamstrahlung effects are included. Therefore we restrict ourselves to the bremsstrahlung process in most of the cases and try to select it from all the background expected to contribute.

The bremsstrahlung process admits two main strategies for the Higgs search:

- calculation of the mass recoiling against the Z^0, most conveniently applied in the $Z^0 \longrightarrow e^+e^-$ and $\mu^+\mu^-$ decay modes. This method has the unique feature of being independent on assumptions about the Higgs decay modes;
- direct reconstruction of the invariant mass of the Higgs decay products; here the decays $H^0 \longrightarrow b\,\bar{b}$, WW, $\tau\bar{\tau}$ and light $q\,\bar{q}$ or $g\,g$ are appropriate, with the $b\,\bar{b}$ decay mode being the most effective one for the H^0 discovery, and, if possible, the fusion processes are included.

In the past, various H^0 analyses have been developed for practically all possible H^0 and Z^0 decays, see e.g. [19, 20, 21]. Here, we follow the guidelines of

these studies, but have either improved the selection criteria or added further restrictions or impose energy-momentum as well as $M(l^+l^-) = M(Z^0)$ constraints, when appropriate, in order to achieve better experimental resolution. If for a particular H^0 and Z^0 decay a set of cuts and constraints had been established, all reactions of Table 2 were also processed under these conditions. Their contributions to either the recoil mass or the appropriate invariant mass were added so that the Higgs signal over the corresponding background can be explored.

Higgs signal topologies expected are shown in Fig.2. Typically the associated

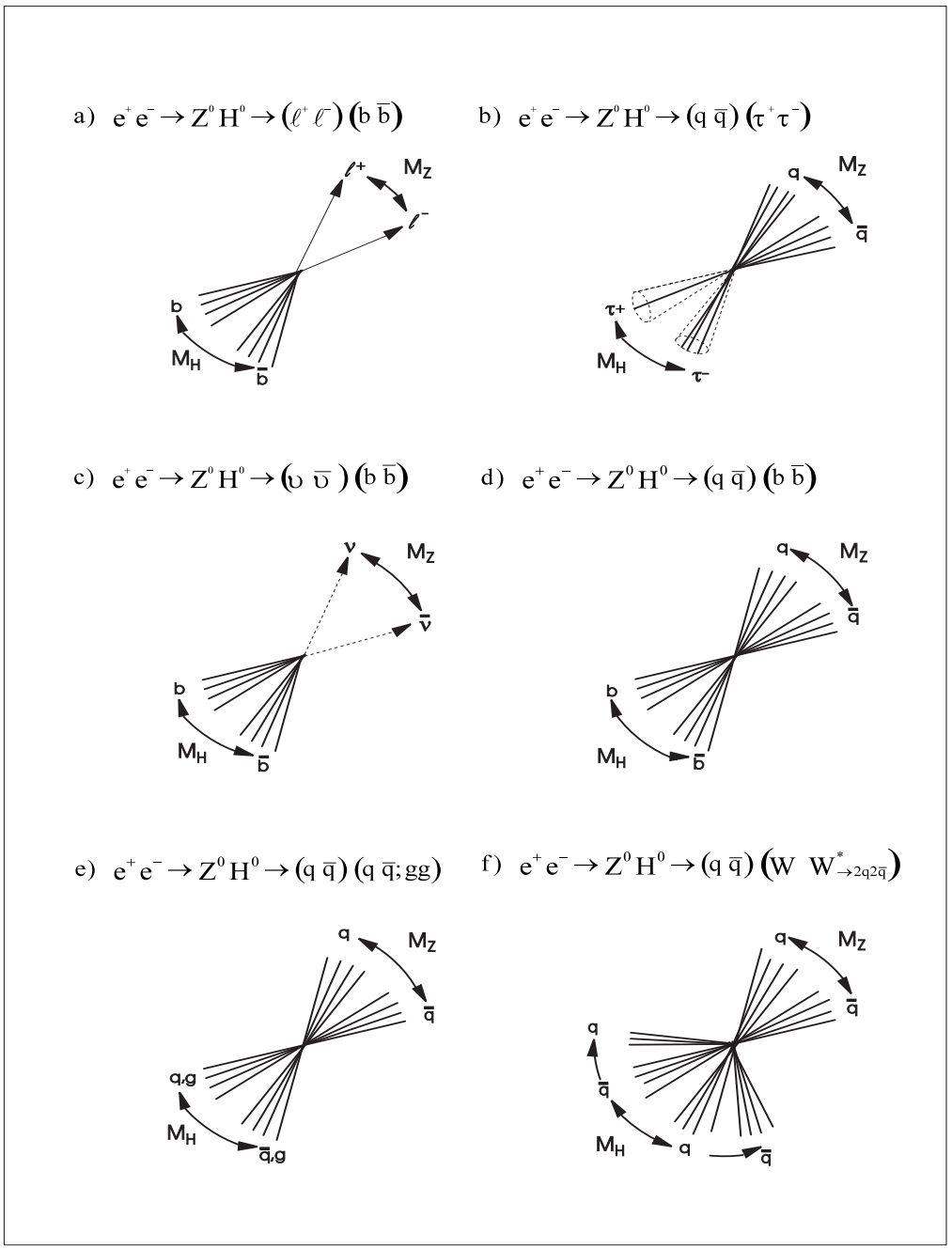

Figure 2: *Higgs signal topologies expected for the reactions studied in this paper.*

$e^+e^- \longrightarrow Z^0\ H^0$ production is followed by the decay of the $Z^0 \longrightarrow l\bar{l}$ (10%), $\nu\bar{\nu}$ (20%), $q\,\bar{q}$ (70%) and the decay of the H^0 mostly into $b\,\bar{b}$, WW^* and occasionally into $\tau^+\,\tau^-$ or into light quarks $q\,\bar{q}$ and two gluons. Only $W \to q\bar{q}$ decays are considered here.

For each of the reactions we apply so-called standard and improved cuts so that the background is removed to a negligible (or acceptable) level while the signal is retained to a large extent. Standard cuts are mainly introduced to suppress non-high $p_\perp$, low-multiplicity events whereas the improved cuts are chosen to remove effectively WW and $q\bar{q}$ pairs as well as $e\nu W$, WWZ and ZZZ background contributions and possible reflections of any of the signal channels (1) - (5), (9) onto that one under study. The numbers of signal and background events, S and B, are then counted in a window around the Higgs mass in order to determine the statistical significance $S/\sqrt{B}$ of the signal. This quantity is studied as a function of the accumulated luminosity and, if $S/\sqrt{B}$ is typically 5 or larger, Higgs detection should be promtly feasible either in the recoil mass or in the invariant mass of its decay products. It is worthwhile to note that the proposed criteria are robust and relatively simple, and they are not optimized such that significant improvements are expected to be possible once the detailed detector behaviour is known. Our concern today is to demonstrate the potential of Higgs discovery at the NLC by the analysis methods proposed here.

5.1 The leptonic channel: $e^+e^- \longrightarrow Z^0\ H^0 \longrightarrow (\mu^+\mu^-\ ;e^+e^-\ )(b\,\bar{b}\ )$

According to the topology in Fig.2a, the Higgs can be detected either by calculating the recoil mass, $M^2_{rec} = s - 2\sqrt{s}E_Z + M^2_Z$, once two-opposite charged leptons with invariant mass close to the Z^0 mass are identified, or by investigation of the hadronic 2-jet mass.

The set of cuts we have adapted to analyze this channel consists of

a) the total transverse energy of the event has to be larger than 30 GeV but less than 250 GeV;

b) the total momentum along the beam is restricted to be within the range $\pm$ 120 GeV;

c) the visible energy of the event should be larger than 230 GeV;

d) the total number of tracks exceeds 14;

e) $M(\mu^+\mu^-\ ) = M_Z \pm$ 10 GeV, respectively, $M(e^+e^-\ ) = M_Z \pm$ 6 GeV, with $|cos\Theta_Z| < 0.8$;

f) if the Z^0 decays into two muons, the energy of isolated electrons has to be smaller than 25 GeV, whereas for $Z^0 \longrightarrow e^+e^-$ decays, the electron energy is required to be between 10 and 140 GeV;

g) if the hadronic system contains two jets[1] with an opening angle larger than 40^o, each jet has to have an energy larger than 10 GeV, a number of particles of at least 5 and $|cos\Theta_{jet}| < 0.8$;

h) the number of tracks with large impact parameter, b_{norm} $\geq$2, has to be larger or equal than 3; here, the Z^0 deay products are not acounted for.

Conditions a) - d) are very useful to reject most of low $p_\perp$, low-multiplicity background; they do not remove signal events. Constraint f) aims to suppress (irreducible) background from the reaction $e^+e^- \longrightarrow e^+e^- q\,\bar{q}$. The remaining criteria are chosen to isolate H^0 events from the overwhelming WW and $q\,\bar{q}$ (γ) background, to ensure good particle measurability and to enrich $H^0 \longrightarrow b\,\bar{b}$ decays. In the case of the recoil mass, we applied in addition the constraint M($l\bar{l}$) = M(Z^0) to improve the $S/\sqrt{B}$ ratio.

After all cuts applied we are left with 38% of signal events for further analyses. The determination of the integrated luminosity needed to observe the Higgs with $S/\sqrt{B} \geq 5$ results, for example, in the histograms of Figs.3a and b. Here, the recoil mass as well as the 2-jet mass are shown for 10 fb^{-1} accumulated luminosity, with either 21 or 23 H^0events in the range $M_H \pm^{20}_6$ GeV, respectively, $M_H \pm^{10}_{15}$ GeV over a very small background (of about 2 events).

A non-gaussian behaviour of the reconstructed masses is observed: the recoil mass has a tail on the large side due to ISR and beamstrahlung energy degradation, while the 2-jet mass indicates a tail to the lower side due to imperfect detector acceptances and neutrinos in the final state.

5.2 The tauon channel: $e^+e^- \longrightarrow Z^0\,H^0 \longrightarrow (q\,\bar{q}\ )(\tau^+\,\tau^-\ )$

Since one of our interests is to measure the branching fraction BF (H $\longrightarrow \tau^+\,\tau^-$) from the 4-body final state $\tau^+\,\tau^-\,q\,\bar{q}$ only events with $Z^0 \longrightarrow q\,\bar{q}$ and $H^0 \longrightarrow \tau^+\,\tau^-$decays are selected. This event rate is about two times more abundant than the complementary rate with $Z^0 \longrightarrow \tau^+\,\tau^-$ and $H^0 \longrightarrow q\,\bar{q}$ decays. Accordingly, Higgs detection is possible by inspection of the $\tau^+\,\tau^-$ mass and, once the $Z^0 \longrightarrow q\,\bar{q}$ decay is established, of the mass recoiling against the Z^0 . The final state of interest here is formed by two isolated energetic tau's and two jets as indicated in Fig. 2b.

[1]The LUCLUS[15] jet finding algorithm has been used in this study.

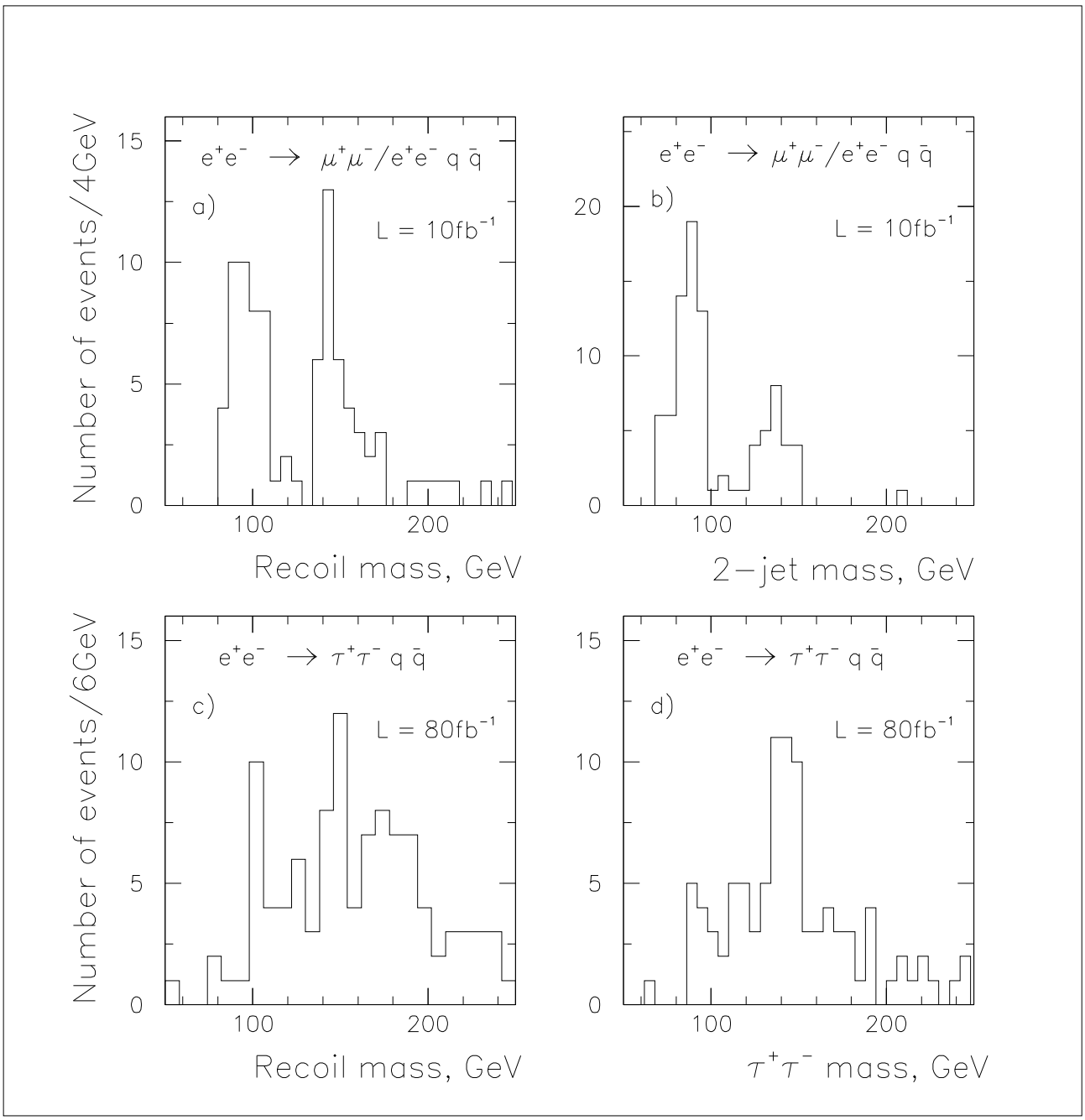

Figure 3: *Recoil and 2-jet ($\tau^+\tau^-$) mass distributions for the reactions $e^+e^- \longrightarrow \mu^+\mu^-/e^+e^- q\bar{q}$ and $\tau^+\tau^- q\bar{q}$ with integrated luminosities as indicated. Background contributions are included.*

In order to distinguish a possible signal from all background contributions we apply at first the following cuts:

a) the total transverse energy of the event should be in the range 30 GeV to 240 GeV;

b) the total momentum along the beam is restricted to be within $\pm$140 GeV;

c) the visible energy of the event is larger than 150 GeV but below 330 GeV,

to allow for missing energies by neutrinos from τ decays;

d) the number of charged particles should exceed 8;

e) isolated electrons with a polar angle between 15^0 and 165^0 should have an energy less than 125 GeV.

The two τ's are selected as the two most isolated oppositely charged particles[2] with

f) a transverse momentum of at least 3.5 GeV;

g) no other charged particles in a cone of 25^0 around their direction;

h) not identified as an e^+e^- or $\mu^+\mu^-$ pair;

i) all neutrals within a cone of 12.5^0 around the charged particle direction are included.

The particles selected by criteria f) - i) are then subtracted from the event and the remainder is considered to be a 2-jet system with an invariant mass within 15 GeV of the Z mass. Since we know the cm energy and momentum, the initial τ and jet energies are recomputed by a fit; otherwise no H^0 signal would be visible in the recoil and the $\tau^+\,\tau^-$ mass spectra.

In order to ensure good event containment, reasonable track reconstruction capability, well-defined $Z^0 \longrightarrow$ 2-jet decays and suppression of ZZ events we require additionally

j) the χ^2,
$\chi^2 = \frac{(M_Z - M_{jj})^2}{\sigma^2_{M_{jj}}} + \frac{(M_H - M_{\tau\tau})^2}{\sigma^2_{M_{\tau\tau}}}$,
is less than 25. The σ's are the corresponding mass resolutions;

k) $|cos\Theta_Z| < 0.8$;

l) the two jets found should have an opening angle larger than 40^o and, for each jet, it is demanded to have an energy larger than 10 GeV, $|cos\Theta_{jet}| < 0.8$ and to involve at least 5 particles.

Some 15 % of the signal events survive all cuts. However, non-negligible background remains due to insufficient ZH particle association from the $\tau^+\,\tau^-\,q\,\bar{q}$ final state and due to WW pair and $2q2\bar{q}$ background production. In addition, the small H $\longrightarrow \tau\tau$ branching fraction of 4.5 % together with degraded mass resolutions makes a Higgs discovery in the $\tau\tau q\,\bar{q}$ channel not easy. Large statistics

[2]For simplicity, only 1-prong τ decays are considered.

and well-educated selection procedures are prerequisites to observe a convincing signal. The results of our analysis for 80 fb^{-1} integrated luminosity are shown in Figs. 3c and d. In the $\tau^+\,\tau^-$ mass distribution a clear signal of $\sim$ 22 events over 10 background events is expected in the mass range $M_H \pm$ 12 GeV, whereas the recoil mass seems to be less useful for finding the Higgs.

5.3 The missing energy channels: $e^+e^- \longrightarrow Z^0\,H^0 \longrightarrow (\nu\bar{\nu}\,)(b\,\bar{b}\;)$ and $e^+e^- \longrightarrow \nu\bar{\nu}\,H^0 \longrightarrow \nu\bar{\nu}\,(b\,\bar{b}\;)$

The missing energy channel is of great interest because of its potentially large discovery potential for the Higgs with limited integrated luminosity, due to the existence of two signal diagrams and the large branching fractions BF($Z^0 \longrightarrow \nu\bar{\nu}$) and BF($H^0 \longrightarrow b\,\bar{b}\;$).

The topology expected is an (acoplanar) pair of jets accompanied by large missing energy. The difference between the two H^0 production mechanisms consists basically in the constraint M($\nu\bar{\nu}\,$) = M$_Z$, which might be applied to select the bremsstrahlung process, see Fig.2c. The isolation criteria we have used to select the signal from background processes are:

a) the total transverse energy of the event should be larger than 10 GeV but less than 170 GeV;

b) the total momentum along the beam line is within the range $\pm$ 140 GeV;

c) the visible event energy is larger than 50 GeV and less than 210 GeV, to allow for large missing energy;

d) the number of charged particles is larger than 6;

e) isolated electrons have an energy smaller than 50 GeV and their polar angle should be between 20^o and 160^o;

f) the invisible mass recoiling against the 2-jet system has to be within 60 and 250 GeV;

g) the hadronic system involves two jets with an opening angle of at least 30^o;

h) each jet should have an energy larger than 10 GeV, involves at least 5 particles and has a polar angle with $|cos\Theta_{jet}| < 0.8$;

i) the number of tracks with large impact parameter, b$_{norm} > 3$, is required to be 5 or larger.

Cuts a) - e) reduce background to a large extent; they do not remove signal events significantly. The other criteria should accumulate well-defined b-quark jets. Note that we have strengthened the definition for 'large impact parameter' track with the result that remaining W^+W^-, eνW, $q\,\bar{q}\ (\gamma)$ and $e^+e^-\,q\,\bar{q}$ background rates are reduced to a very small level.

After application of all criteria, 36 % of the signal events survive which, together with the relatively large cross sections for the bremsstrahlung and fusion processes times the corresponding Z^0 and H^0 branching fractions, allows to reduce the integrated luminosity to 1 fb^{-1} to observe 8-9 signal events over about 3 background events within the mass range 120 to 145 GeV, as can be seen in Fig.4. Due to fluctuations expected within such small event samples we conclude that 1.5 to 2 fb^{-1} of accumulated luminosity should be sufficient to observe a significant signal. This result makes the $\nu\bar{\nu}\,q\,\bar{q}$ channel very attractive for a quick Higgs search in e^+e^- collisions at cm energies of $\sim$ 300 to 360 GeV.

5.4 The 4-jet channel: $e^+e^- \longrightarrow Z^0\,H^0 \longrightarrow (q\,\bar{q}\ )(b\,\bar{b}\ )$

The topology of this channel (Fig. 1d) involves 4 jets from the $Z^0 \longrightarrow q\,\bar{q}$ and $H^0 \longrightarrow b\,\bar{b}$ decays. Again, two possibilities for the Higgs search exist; the recoil mass and the $b\,\bar{b}$ invariant mass can be searched for a signal. Since numerous backgrounds are expected to contribute to this topology a more sophisticated analysis has to be developed. We have come up with the following selection criteria:

a) the total transverse energy of the event should be larger than 30 GeV and smaller than 270 GeV;

b) the total momentum in beam direction has to be in the range $\pm$ 120 GeV;

c) the visible energy exceeds 180 GeV;

d) the number of charged particles should be larger than 24;

e) isolated electrons should have a polar angle between 20^o and 160^o and an energy smaller than 60 GeV;

f) the event is accepted if the number of jets found equals 4 and the opening angle between any pair is larger than 20^o;

g) from all possible Z and H jet pairing only the combination with smallest χ^2,
$\chi^2 = \frac{(M_Z - M_{ij})^2}{\sigma^2_{M_{ij}}} + \frac{(M_H - M_{kl})^2}{\sigma^2_{M_{kl}}}$,

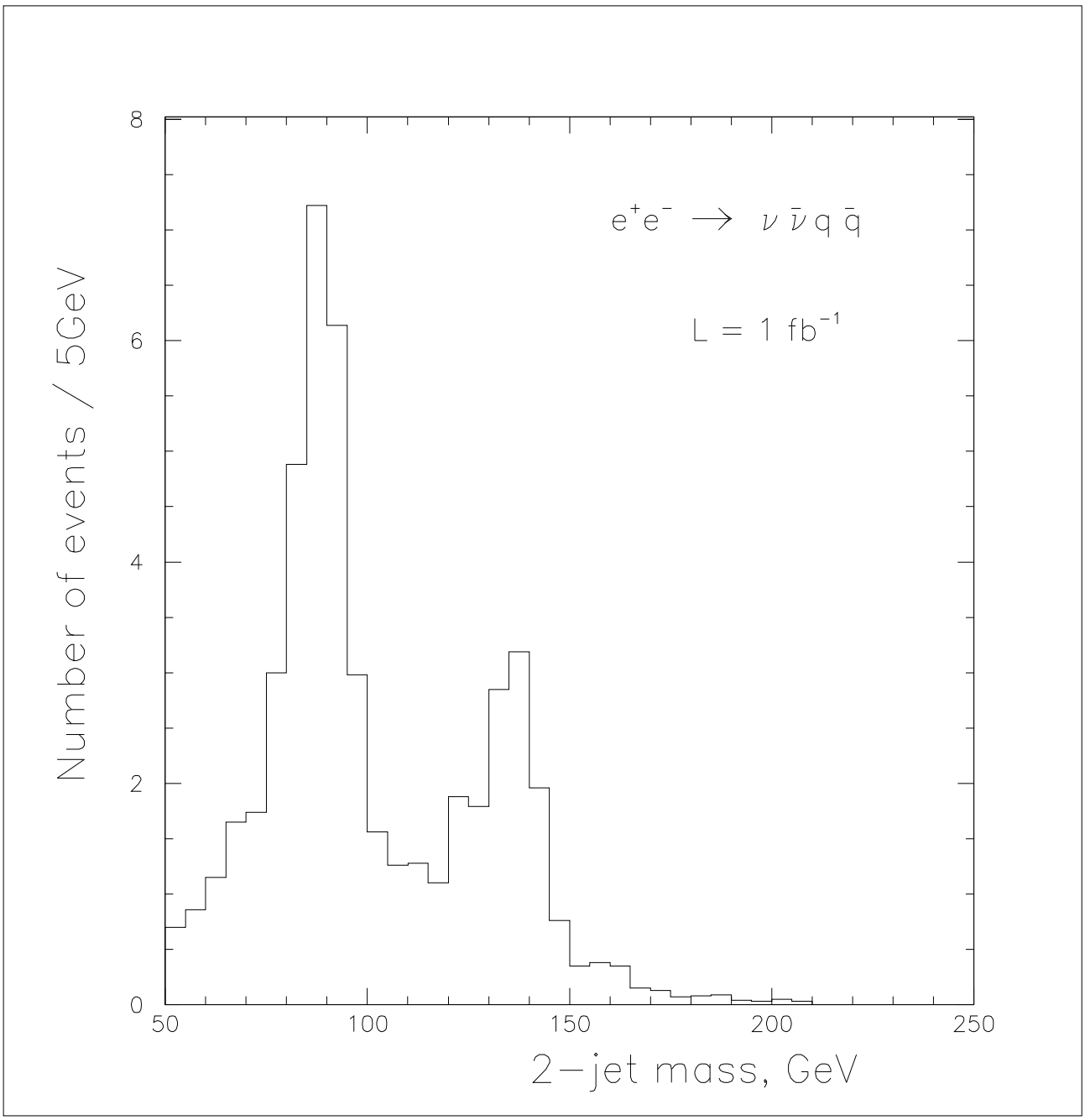

Figure 4: *2-jet mass distributions of the reaction* $e^+e^- \longrightarrow \nu\bar{\nu}\,q\,\bar{q}$ *for an integrated luminosity of 1* fb^{-1}. *Background contributions are included.*

is selected. M_{ij} is the invariant mass of the jet-pair (i,j) and $\sigma_{M_{ij}}$ is its mass resolution;

h) the four jet energies are recomputed using energy-momentum conservation, while keeping their directions at measured values;

i) the polar angle of the 2-jet system consistent with the Z^0 is restricted to $|cos\Theta_Z| < 0.8$;

j) each jet should have an energy larger than 10 GeV, $|cos\Theta_{jet}| < 0.8$ and contains at least 5 particles;

k) the number of tracks with significant impact parameter, $b_{norm} > 3$, is 5 or larger.

Criteria a) - e) remove low-$p_\perp$, low-multiplicity background while retaining most of the signal events. Cuts f) and g) ensure a 4-jet topology with the best Z H interpretation. The remaining conditions take care of a good event containment, reasonable jet properties and b-quark enrichment. After all cuts, 18% (9%) of the signal remains in the 2-jet (recoil) mass distribution. The smaller efficiency for the recoil mass is caused by the additional constraint that the mass of the 2-jet system recoiling against the Higgs has to be within $M_Z \pm$ 15 GeV. For an integrated luminosity of 3 fb^{-1} we expect 23 H^0 events over $\sim$ 5 background events in the 2-jet mass range $M_H \pm$18 GeV (Fig.5b), whereas 15 signal events over $\sim$ 3 background events are observed in the recoil mass within the range $M_H \pm^{12}_{30}$ GeV, as seen in Fig.5a. The surviving background is practically due to WW pair production only.

5.5 The 6-jet channel: $e^+e^- \longrightarrow Z^0\,H^0 \longrightarrow (q\,\bar{q}\ )(WW^*) \longrightarrow (q\,\bar{q}\ )(2q2\bar{q})$

Due to the large branching fraction of the Higgs into WW* expected for M_H = 140 GeV and its sensitivity to discriminate between SM-like and non SM-like Higgs particles , it is highly interesting to know which luminosity is needed to observe a statistically significant $H^0 \longrightarrow$ WW* signal. The event selection, however, becomes now more complicated as can be anticipated from the expected topology shown in Fig. 1f. Here, we consider only hadronic decays of the vector bosons taking into account the advantage of their large branching fractions. An analysis including also the leptonic W $\longrightarrow l\nu$ decay may be found in [21], with the result that only a marginal signal could be extracted.

As mentioned in sect.4, the absence of a 2-to-6 body event generator needed for a general analysis analogous to that of sects. 5.1 to 5.4, implies to proceed as in previous Higgs studies, namely computing production cross section times branching fractions. Events of the signal reaction $e^+e^- \longrightarrow Z^0H^0 \longrightarrow (q\,\bar{q}\ )$(WW*) $\longrightarrow (q\,\bar{q}\ )(2q2\bar{q})$ are generated and confronted with the expectations from reactions (1)-(8), (13) and (14) and the 6-jet channels $e^+e^- \longrightarrow$ WWZ, ZZZ $\longrightarrow 3q3\bar{q}$, which are believed to be the significant sources of background.

The analysis requires the reconstruction of 6-jet final states containing four jets from the Higgs and two from the Z. Basically, the signal can be searched for either in the WW* ($\longrightarrow 2q2\bar{q}$) invariant mass or in the recoil mass against the identified Z^0 . The following criteria have been applied in our analysis:

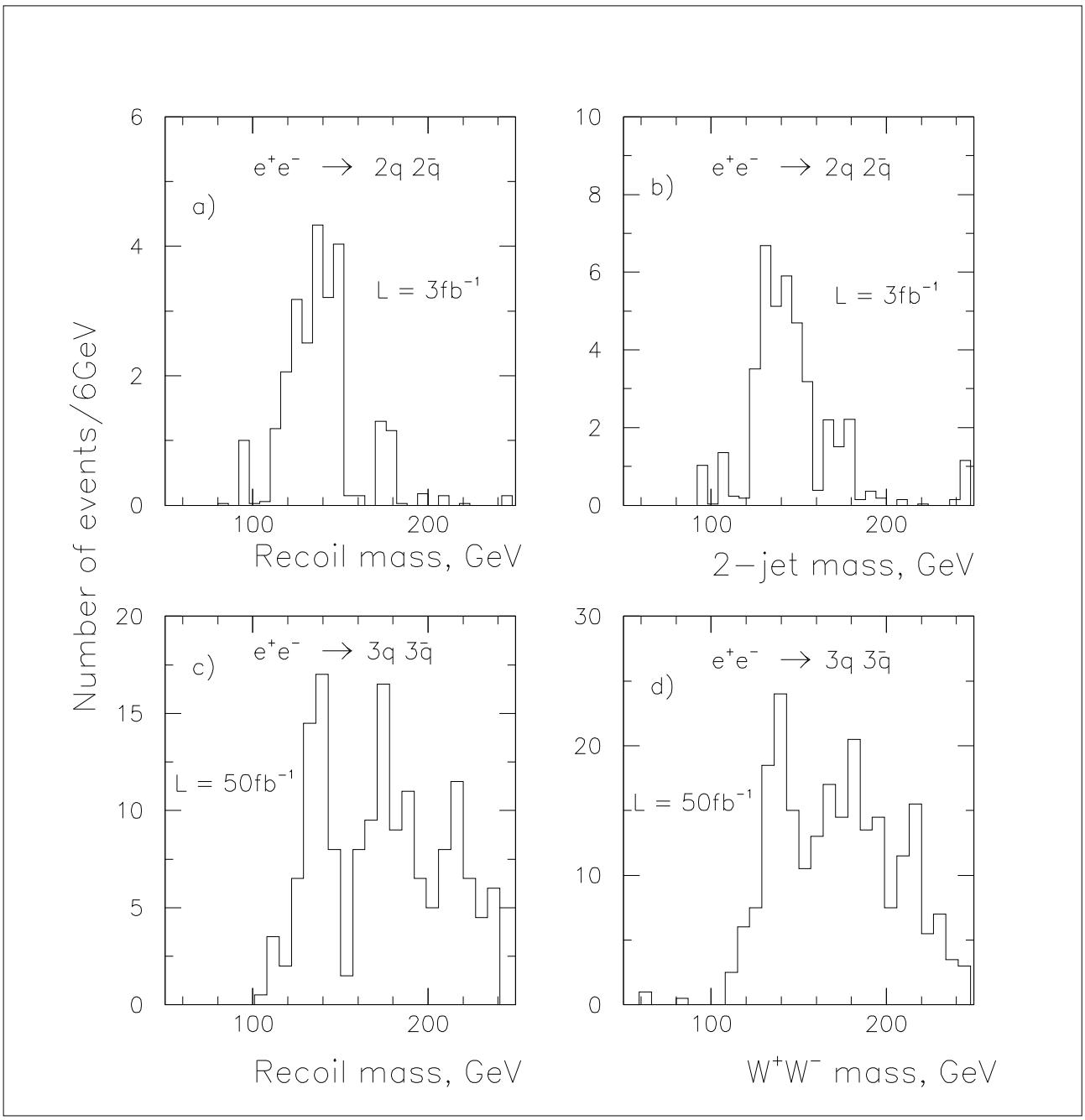

Figure 5: *Recoil mass and 2-jet (WW^*) mass distributions for the reactions $e^+e^- \longrightarrow 2q2\bar{q}$ and $3q3\bar{q}$ with integrated luminosities as indicated. Background contributions are included.*

a) the transverse energy of the event should be larger than 50 GeV and below 270 GeV;

b) the total momentum in beam direction is restricted to $\pm$ 80 GeV;

c) the visible event energy is larger than 220 GeV;

d) the number of charged particles exceeds 25;

e) isolated electrons should have an energy smaller than 30 GeV and a polar

angle in the range 12^0 to 168^0;

f) the thrust is restricted to be in the range 0.60 to 0.90;

g) if the event involves 6 jets, the opening angle between any two of them has to be larger than 20^0;

h) for each jet it is required to have an energy larger than 10 GeV, $|cos\Theta_{jet}| < 0.8$ and to involve at least 5 particles;

i) from all possible Z and H jet pairing only the combination with smallest χ^2,
$\chi^2 = \frac{(M_Z - M_{ij})^2}{\sigma^2_{M_{ij}}} + \frac{(M_H - M_{klmn})^2}{\sigma^2_{M_{klmn}}} + \frac{(M_W - M_{kl})^2}{\sigma^2_{M_{kl}}}$,
is selected. M_{ij} (M_{klmn}) is the invariant mass of the jet system (i,j) (k, l, m, n) and the σ's are the corresponding mass resolutions;

j) the jet energies are recomputed using energy-momentum conservation, while keeping their directions at measured values;

k) the polar angle of the 2-jet pair consistent with the Z^0 is restricted to $|\cos\Theta_Z| < 0.8$;

l) the event is rejected if more than 4 tracks with significant impact parameter, $b_{norm} > 3$, are found (anti-b tag).

Low-$p_\perp$, low-multiplicity background is rejected by criteria a) - e), while practically all signal events are retained. Once the event has been selected as a ZH final state by the χ^2 condition, cuts for jet containment and good jet properties are applied. In order to remove background from Higgs decays to $b\,\bar{b}$, an anti-b tag is required.

After all cuts applied, 7.5 % and 6.3 % of the signal survives in the 4-jet mass respectively recoil mass distribution. The background left is mainly due to WW pair and $2q2\bar{q}$ production, in the ratio of about 15 : 1. An integrated luminosity of 50 fb^{-1} would allow to observe 32 H^0 events over a background of ~ 18 in the 4-jet mass distribution, as shown in Fig. 5d. The recoil mass spectrum would yield a signal of 30 events over ~ 9 background events. The events counted are within the mass ranges $M_H \pm^6_{12}$ GeV respectively $M_H \pm 12$ GeV. Finally, we notice that the 6-jet background not accounted for in this study is expected not to alter our conclusions significantly.

5.6 The light quarks and gluon channels: $e^+e^- \longrightarrow Z^0\,H^0 \longrightarrow (\nu\bar{\nu}\,)(c\bar{c}$ + gg), $e^+e^- \longrightarrow \nu\bar{\nu}\,H^0 \longrightarrow \nu\bar{\nu}\,(c\bar{c}$ + gg) and $e^+e^- \longrightarrow Z^0\,H^0 \longrightarrow (q\,\bar{q}\;)(c\bar{c}$ + gg)

The search for Higgs decays into lighter quarks and gluons takes advantage of the existence of several production processes. Either the missing energy channel with Higgs production via the bremsstrahlung or the fusion mechanism can be searched for or the 4-jet topology with $Z^0 \longrightarrow q\,\bar{q}$ and $H^0 \longrightarrow c\bar{c}$ + gg decays can be used. Since the SM branching fraction for 140 GeV Higgs into $c\,\bar{c}$ is only 1.5%, we have combined the $c\bar{c}$ and gg decay modes, resulting in a 6.4% decay fraction[3].

The encouraging Higgs discovery potential of the 2-jet missing energy channel (4) involves to some extent Higgs decays into lighter quarks, but only at a very small level. Here, we focus on a a strategy to select $H^0 \longrightarrow c\bar{c}$ + gg decays out of the huge background expected. In principle, the 2-jet missing energy channel should not considerably suffer from WW pair or any other background contributions, because two and only two jets and large missing energy in the final state are required. However, it has been found that very stringent selection criteria are needed to distinguish a possible signal from the remaining background:

a) the total transverse energy has to be in the range 30 to 150 GeV;

b) the total longitudinal momentum is restricted to $\pm$ 120 GeV;

c) the visible event energy is larger than 140 GeV and less than 210 GeV;

d) isolated electrons with a polar angle between 30^o and 150^o should have an energy less than 5 GeV;

e) the number of charged particles per event is larger than 15;

f) the thrust is required to be below 0.9;

g) the hadronic system involves two jets with an opening angle of at least 80^o;

h) each jet should have an energy larger than 30 GeV, $|cos\Theta_{jet}| < 0.7$ and involves more than 11 particles;

i) the missing mass has to be consistent with the Z^0 mass;

j) the number of tracks with large impact parameter, $b_{norm} > 3$, is less than 4 to suppress $H^0 \longrightarrow b\,\bar{b}$ events (anti-b tag).

[3]It would be very desirable to measure the $H^0 \longrightarrow c\bar{c}$ decay fraction separately. This requires, however, very large statistics and an excellent vertex detector to collect a relatively clean $c\bar{c}$ event sample

Fig.6 shows the combined 2-jet mass distribution for the signal and the surviving background events, for 100 fb^{-1} integrated luminosity. The shaded histogram

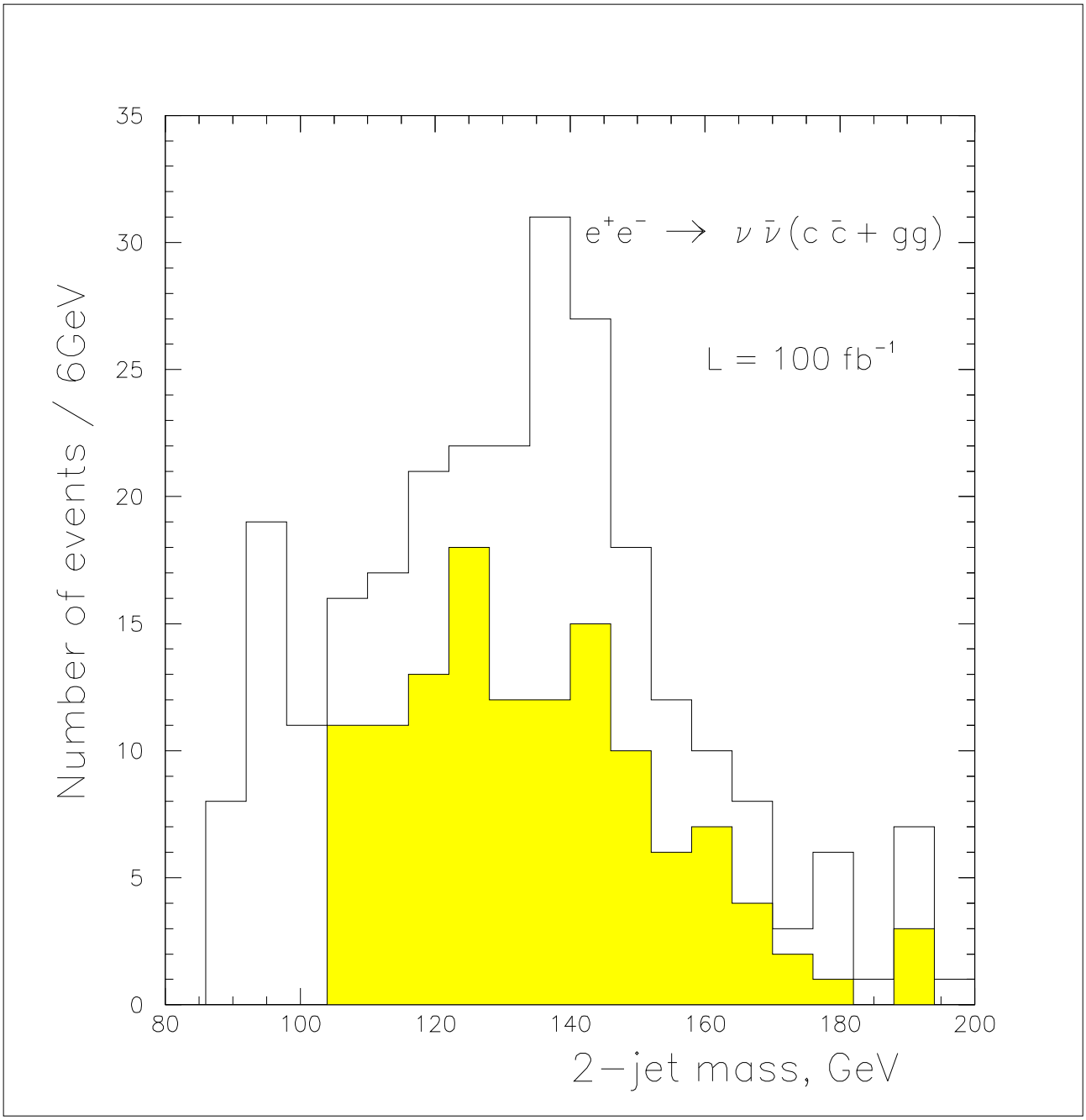

Figure 6: *2-jet mass distribution of the reaction $e^+e^- \longrightarrow \nu\bar{\nu}$ ($c\bar{c}$ + $g\,g$) for an integrated luminosity of 100 fb^{-1}. The shaded histogram represents the reducible background expected.*

represents the reducible background, mainly from WW pair production and, to lesser extent, from the $\tau^+\,\tau^-\,q\,\bar{q}$ channel. As can be seen, a signal of about 40 H^0 events exists on $\sim$ 60 events of background within 12 GeV of the Higgs mass. Although $S/\sqrt{B}$ is somewhat below 5 we consider it as convincing and as a demonstration to observe $H^0 \longrightarrow c\bar{c}$ + gg decays.

In the case of the 4-jet event topology, all our attempts to select a clean

H^0 signal were unsuccessful. We were not able to establish a set of criteria to reject most of the ZZ and WW background and more refined constraints have to be developed in order to make a signal-to-background analysis successful.

6 Branching fractions of the Higgs boson

If a Higgs boson is discovered, it is imperative to understand its nature. Besides its mass the parameters which determine the relation of the Higgs to the Standard Model are its couplings to vector bosons and fermions. The reactions studied (see Table 1) allow to determine the branching fractions for $H^0 \longrightarrow b\,\bar{b}$, $\tau^+\,\tau^-$, WW and light $q\,\bar{q}$ + gg decays.

Let us consider, as an example, the reaction $e^+e^- \longrightarrow Z^0\,H^0 \longrightarrow \mu^+\mu^-\;b\,\bar{b}$. From the reconstructed $b\,\bar{b}$ invariant mass the quantity $\sigma(ZH)_{tot}\cdot$ BF($Z^0 \longrightarrow \mu^+\mu^-$)$\cdot$ BF($H^0 \longrightarrow b\,\bar{b}$) can be measured. The branching fraction of the Z^0 to $\mu^+\mu^-$ is well known from LEP experiments so that in order to obtain BF ($H^0 \longrightarrow b\,\bar{b}$) and its error one has to measure the inclusive Higgs bremsstrahlung cross section $\sigma(ZH)_{tot}$ and to compute

$$BF(H^o \rightarrow b\bar{b}) = \frac{[\sigma(ZH)_{tot} \cdot BF(H^o \rightarrow b\bar{b})]}{\sigma(ZH)_{tot}} \tag{18}$$

6.1 The inclusive cross section $\sigma(ZH)_{tot}$

The measurement of the inclusive $e^+e^- \longrightarrow Z^0\,H^0$ cross section is based on the selection of all Z's produced in an e^+e^- experiment, with decays into muon and electron pairs. If any $\mu^+\mu^-$ or e^+e^- pair detected has a mass consistent with the Z^0 mass its recoil mass is calculated and plotted. From this spectrum $\sigma(e^+e^- \longrightarrow Z^0\;H^0\;)_{tot}$ and its error can be estimated taking into account the dilepton Z^0 branching fraction, acceptance and resolution effects of the detector and the impact of ISR and beamstrahlung.

For all reactions studied so far together with the additional signal channel $e^+e^- \longrightarrow Z^0\,H^0 \longrightarrow (\mu^+\mu^-; e^+e^-)$(WW*) and allowing for all W decay modes, we show in Fig.7 the recoil mass expected against all dilepton pairs with M($\mu^+\mu^-$) = $M_Z \pm$ 10 GeV and M(e^+e^-) = $M_Z \pm$ 6 GeV and $|cos\Theta_Z| < 0.8$. Some improvement of the recoil mass resolution has been achieved by the constraint M($l\bar{l}$) = M_Z since it is essential that the peak be as narrow as possible in order to enhance the signal-to-background ratio. The cut applied on the Z^0 polar angle is demanded in order to reduce large background from s-channel Z/γ^* (see Fig. 1a) and $Z^0\,Z^0$ events. The Higgs signal, summed over all its decays, is clearly visible. It has a non-gaussian shape which is caused by loss of energy in the

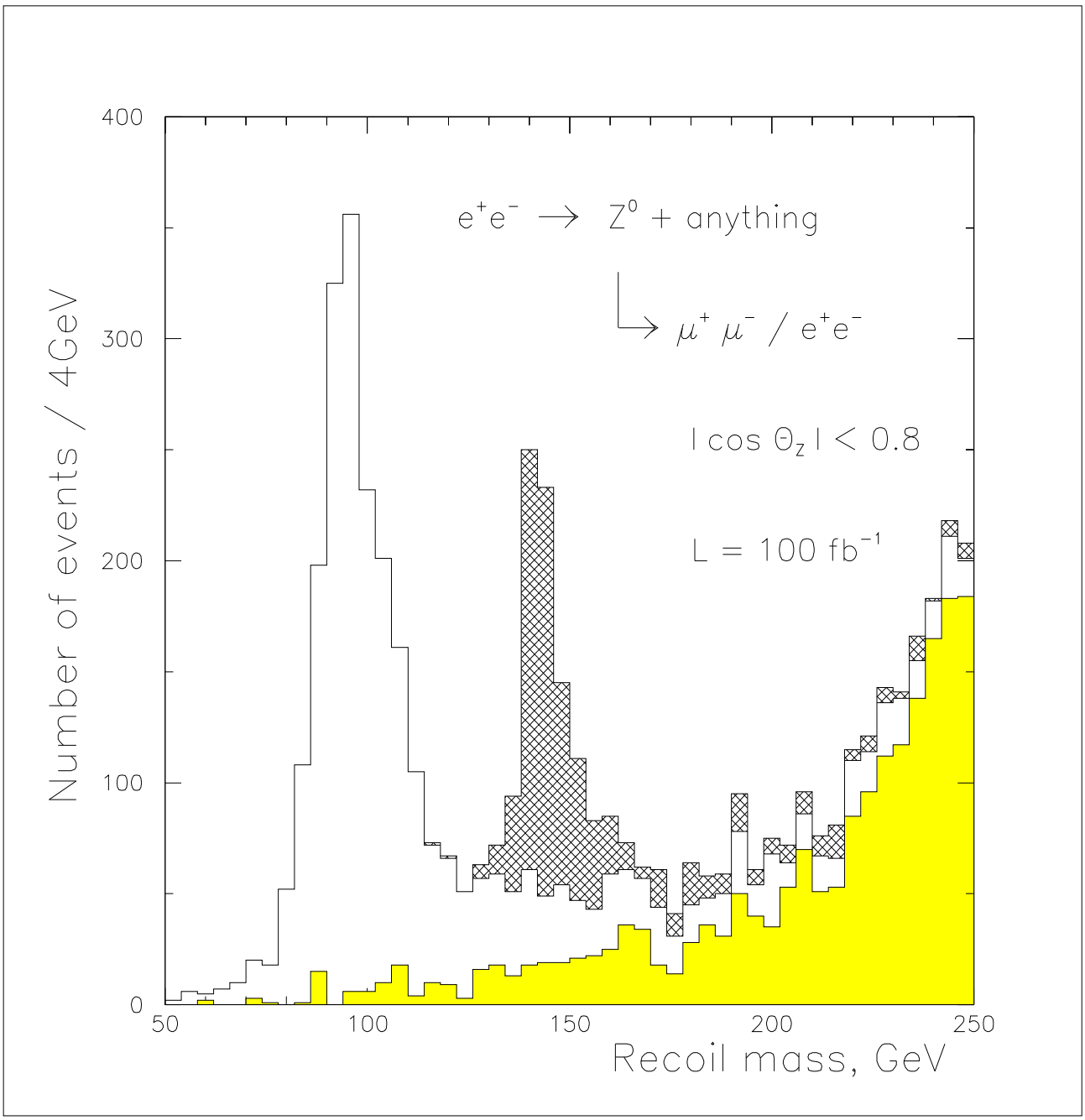

Figure 7: *Inclusive recoil mass distribution in the process* $e^+e^- \longrightarrow Z^0$ ($\longrightarrow \mu^+\mu^-$ /e^+e^-) + *anything for an integrated luminosity of 100* fb^{-1} *and* $|cos\Theta_Z| < 0.8$. *The shaded histogram represents the reducible background expected, whereas the Higgs contribution is shown cross-hatched. The irreducible background for the* $H^0 \longrightarrow WW$ *channel has been neglected.*

initial state due to photon radiation and beamstrahlung resulting to a reduced peak hight and a long tail on the high mass side. The remaining reducible background, mainly due to WW pair and e^+e^- /$\mu^+\mu^-(\gamma)$ production, is shown as hatched histogram in Fig. 7. In the recoil mass range 138 to 154 GeV we expect 533 H^0 events over $\sim$ 181 background events, so that the statistical precision of the inclusive H^0 signal, $\sqrt{S+B}/S$, is $\pm$ 5%. This accuracy should also hold for

the HZZ coupling-squared which is proportional to $\sigma(ZH)_{tot}$.

6.2 Measurement of the Higgs branching fractions

In the following we assume the SM couplings of the Higgs particle to bosons and fermions, a statistical error of 5% for the inclusive Higgs production cross section $\sigma(ZH)_{tot}$ and determine the statistical error of the branching fraction BF($H^0 \longrightarrow$ xx), for each of the possible $H^0 \longrightarrow$ xx decay mode.

The branching fraction BF(H $\longrightarrow b\,\bar{b}$) can be determined from three processes, $e^+e^- \longrightarrow l\bar{l}\,b\,\bar{b}$, $\nu\bar{\nu}\,b\,\bar{b}$ and $q\,\bar{q}$ $b\,\bar{b}$. Because of the different statistics and systematics expected in these channels, we measure this fraction for each reaction separately and then combine the results.

The process $e^+e^- \longrightarrow \mu^+\mu^-$;e^+e^- $b\,\bar{b}$ has the advantage of a simple signal extraction with relatively small background. The selection criteria applied (see sect.5.1) allow however for some $H^0 \longrightarrow c\bar{c}$ or other H^0 decays with badly measured tracks. We found 13 non-$b\,\bar{b}$ events and subtracted them from the observed signal in the 2-jet invariant mass resulting to 86 $H^0 \longrightarrow b\,\bar{b}$ events over 18 background events, within the range $M_H \pm^{10}_{15}$ GeV. Hence, a 12 % statistical error for $\sigma(ZH)_{tot}\cdot$ BF(H $\rightarrow b\,\bar{b}$) is obtained from this topology.

The reaction $e^+e^- \longrightarrow \nu\bar{\nu}\,b\,\bar{b}$ benefits from the three times larger branching fraction of the Z^0 into $\nu\bar{\nu}$ w.r.t. muons or electrons and from a topology (Fig. 1c) which is very distinct from many important background reactions. Most of the remaining reducible background is due to WW pair and $e^+e^-\,q\,\bar{q}$ production, where the e^+ and e^- are lost down the beam pipe. However, the background is manageable after application of cuts as proposed in sect.5.3. Taking into account the 16 non-$b\,\bar{b}$ H^0 decays expected and demanding the invisible mass to be close to M_Z, we count 460 $H^0 \longrightarrow b\,\bar{b}$ events over 95 background events, in the mass range $M_H \pm^{6}_{14}$ GeV. This corresponds to a statistical uncertainty of 5.1 % for σ(ZH)$_{tot}\cdot$ BF(H $\rightarrow b\,\bar{b}$).

For the reaction $e^+e^- \longrightarrow 2q2\bar{q}$ four well-defined jets are required in the final state. They have been selected as described in sect.5.4. In order to reduce the considerable WW and large irreducible ZZ contaminations only the jet pairing in best agreement with the Z^0 H^0 hypothesis has been selected. Our analysis, after corrections for non-$b\,\bar{b}$ H^0 decays, results in 479 H^0 $\longrightarrow b\,\bar{b}$ events over a background of 141 events within $M_H \pm^{14}_{18}$ GeV, so that a statistical error of 5.2% is found for σ(ZH)$_{tot}\cdot$ BF($H^0 \longrightarrow b\,\bar{b}$).

The total error obtained after combining the three (independent) reactions must be added in quadrature with the uncertainty for the inclusive Higgs production cross section of 5%. The resulting statistical error found for the branching fraction BF(H $\rightarrow b\,\bar{b}$) is $\pm$ 6.1%.

The measurement of the Higgs branching fraction into $\tau^+\,\tau^-$ turns out to be more difficult. The reasons are i) a small $H^0 \longrightarrow \tau^+\,\tau^-$ decay rate of 3.6 % , ii) the elusive character of the neutrinos from τ decays so that the τ energies cannot be directly measured and iii) more background due to missing final state particle information. Fortunately, since the Higgs is much more massive then the τ, the τ's in the $H^0 \longrightarrow \tau^+\,\tau^-$ decay receive a tremendous boost, so that, to a good approximation, the decay products of the tau's fall into a very narrow cone around its initial direction. A simple rescaling of the τ energies using energy-momentum conservation while keeping their direction at measured values, results, together with the selection criteria of sect.5.2, in a clear $H^0 \longrightarrow \tau^+\,\tau^-$ signal over acceptable background, as seen in Fig. 3d for an accumulated luminosity of 80 fb^{-1}. For L=100 fb^{-1}, we estimate 32 signal events over a background of 15 events, within 12 GeV of the Higgs mass. Hence, the statistical error expected for $\sigma(ZH)_{tot}\cdot$ BF($H^0 \longrightarrow \tau^+\,\tau^-$) would be 21.4 %, which, together with the uncertainty of $\sigma(ZH)_{tot}$, yields an accuracy of $\pm$ 22 % for the branching fraction BF($H^0 \longrightarrow \tau^+\,\tau^-$).

The determination of the branching fraction H $\longrightarrow$ WW* requires (in our case) the reconstruction of six jets in the final state, with four jets from the Higgs and two from the Z^0 . The application of the selection criteria of sect. 5.5 to signal and background reactions yields 46 signal events over 44 background events, in the mass range $M_H \pm^{14}_{18}$ GeV. After corrections for non-WW Higgs decays, we obtain 20.6% for the statistical error of $\sigma(ZH)_{tot}\cdot$ BF ($H^0 \longrightarrow$ WW). If this number is added in quadrature with the error for $\sigma(ZH)_{tot}$, a $\pm$ 22 % statistical uncertainty is measured for the branching fraction of the Higgs into WW.

As has been shown in sect.5.6, it seems possible to extract $H^0 \longrightarrow c\bar{c}$ + gg events out of the 2-jet missing energy event sample. If, within 12 GeV of the Higgs mass, the number of signal events of Fig.6 are corrected for 4 $H^0 \longrightarrow b\,\bar{b}$ events expected, we obtain 37 signal events on a background of 61 events. This yields, after convolution with the uncertainty of $\sigma(ZH)_{tot}$, a $\pm$ 28% statistical error for the branching fraction BF($H^0 \longrightarrow c\bar{c} + gg$).

7 Summary

In this study we have considered the physics potential of the NLC for the Higgs sector, assuming the validity of the Standard Model. In order to make a signal-to-background analysis as meaningful as possible, we have consistently evaluated both signal and background rates at leading order. Our simulation studies include

- the complete matrix elements for the 2-to-4 body processes $e^+e^- \longrightarrow 2f2\bar{f}$ beyond the usual factorization approximation;
- all import SM Higgs decay channels, except H $\longrightarrow$ ZZ*;
- initial state radiation and beamstrahlung;
- a detector response, with parameters of the detector as recently proposed in the 'Conceptual Design Report' for the S-band and TESLA linear collider options;
- all reducible background reactions expected to contribute.

We demonstrate that a Higgs boson with a mass of 140 GeV can be easily discovered in the reaction $e^+e^- \longrightarrow \nu\nu q\,\bar{q}$ within a few days of running of a 360 GeV collider delivering a luminosity of $5 \cdot 10^{33} cm^{-2} sec^{-1}$. Soon after its discovery, the 4-fermion channel $e^+e^- \longrightarrow 2q2\bar{q}$ would establish the Higgs despite of large expected background due to ZZ and WW pair production. The usually considered gold-plated Higgs discovery channel $e^+e^- \longrightarrow \mu^+\mu^-$; $e^+e^-\ q\,\bar{q}$ provides a clean event sample and allows for simple H^0 selection procedures. However, due to the small $Z^0 \longrightarrow l\bar{l}$ branching fraction an integrated luminosity of about 10 fb^{-1} is needed to observe a convincing signal. This reaction has the great advantage of being independent of the Higgs decay modes when the recoil mass technique is used. Furthermore, from the recoil mass spectrum the inclusive Higgs production cross section can be measured with 5% uncertainty for an integrated luminosity of 100 fb^{-1} which in turn allows to determine the HZZ coupling with high precision. Other decay modes of the Higgs, such as $H^0 \longrightarrow$ WW or $\tau^+\,\tau^-$, are unlikely to be useful for its detection. An integrated luminosity of about 50 fb^{-1} (or more) appears necessary to observe statistically significant signals in these channels. We have, to our knowledge for the first time, clearly demonstrated the capability of an e^+e^- collider to detect Higgs decays into lighter quarks and gluons.

For an integrated luminosity of 100 fb^{-1}, we have determined the statistical errors of the Higgs branching fractions to $b\,\bar{b}$, $\tau^+\,\tau^-$, WW$^{(*)}$ and to $c\bar{c} + gg$. The results obtained, convoluted with an 5% error for the inclusive Higgs production cross section, are summarized in Table 3. As can be seen, many of the Higgs decay modes are accessible to experimental consideration and most of the measurements would have an error around 22% or better so that a powerful discrimination between the SM-like Higgs or SUSY-like Higgs can be achieved, even with our relatively simple analysis procedures.

We would like to emphasize once more that for the production and decay channels considered in this paper, only three-level calculations were made and

Branching fraction	Expected error
BF ($H^0 \longrightarrow b\bar{b}$)	$\pm$ 6.1%
BF ($H^0 \longrightarrow \tau^+\tau^-$)	$\pm$ 22%
BF ($H^0 \longrightarrow$ WW*)	$\pm$ 22%
BF ($H^0 \longrightarrow c\bar{c} + gg$)	$\pm$ 28%

Table 3: *Numerical values of the branching fraction errors assuming SM couplings for the Higgs boson with a mass of 140 GeV, a cm energy of 360 GeV and an integrated luminosity of 100* fb^{-1}.

that the selection criteria proposed are not yet optimized such that significant improvements can be expected once the precise detector behaviour is taken into account.

Acknowledgments

We would like to thank our colleagues within the course of the Conceptual Design Report for many discussions. A.Pukhov is acknowledged for his support and help with CompHEP calculations and D.Schulte for providing the TESLA beamstrahlung parameters. S.Sh. also thanks the DESY-Zeuthen TESLA group for the kind hospitality, in particular P.Söding for his interest and support.

References

[1] S. L. Glashow, Nucl. Phys. **22** (1961) 579;
S. Weinberg, Phys. Rev. Lett. **19** (1967) 1264;
A. Salam, Elementary Particle Theory, ed. by N. Svartholm, Stockholm (1968) 367.

[2] P.W. Higgs, Phys. Rev. Lett. **12** (1964) 132and Phys. Rev. **145** (1966) 1156.

[3] e.g. A.Blondel, 28th Internat. Conference on High Energy Physics, Warsaw, July 25-31, 1996.

[4] M. Carena et al., Higgs Physics at LEP II, CERN-96-01.

[5] D. Froidevaux et al., Proceedings of the Large Hadron Collider, Aachen 1990, CERN 90-10.

[6] Conceptual Design Report, in print.

[7] D. Schulte, Thesis, University Hamburg 1996.

[8] E.A. Kuraev and V.S. Fadin, Sov. J. Nucl. Phys. 41 (1985) 466.

[9] E. Boos et al., Moscow State University preprint SNUTP-94-116 and hep-ph/9503280; E. Boos et al., in Proc. of the Xth Int. Workshop on High Energy Physics and Quantum Field Theory, QFTHEP-95, ed. by B.Levtchenko, and V.Savrin, (Moscow, 1995), p.101.

[10] S. Kawabata, Comp. Phys. Commun. **41** (1986) 127.

[11] V. Barger et al., Phys.Rev. D49 (1994) 79;
E. Boos et al., Z.Phys. C61 (1994) 675;
D. Bardin et al., Phys. Letters B344 (1995) 383;
D. Bardin et al., Phys. Letters B375 (1995) 456.

[12] E. Boos et al., Int. J. Mod. Phys. A10 (1995) 2067;
M. Dubinin et al., Phys. Letters B329 (1994) 379.

[13] E. Boos et al., Z.Phys. C64 (1994) 391.

[14] A. Ballestrero et al., Nucl. Phys. **B415** (1994) 265;
E. Boos et al., Z.Phys. C67 (1995) 613.

[15] T. Sjöstrand, Comp. Phys. Commun. **84** (1994) 74.

[16] T. Ohl, Computer Physics Communication 101 (1997) 269.

[17] J. Ellis, M.K. Gaillard and D.V. Nanopoulos, Nucl. Phys. **B106** (1976) 292;
J.D. Bjorken, Proceedings of Summer Institute on Particle Physics, SLAC Report No. 168 (1976), p.1;
B. Ioffe and V. Khoze, Sov. J. Part. Nucl. 9 (1978) 50;
B.W. Lee, C. Quigg and H.B. Thacker, Phys. Rev. **D16** (1977) 1519.

[18] D.R.T. Jones and S.T. Petcov, Phys. Lett. **B84** (1979) 440;
R.N. Cahn and S. Dawson, Phys. Lett. **B136** (1984) 196;
W. Kilian, H. Krämer and P.H. Zerwas, Phys. Lett. **B148** (1984) 367;
G. Altarelli, B. Mele and F. Pitolli, Nucl. Phys. **B287** (1987) 205.

[19] P. Grosse-Wiesmann, D. Haidt and H.J. Schreiber, DESY 92-123A, p17.

[20] P. Janot, preprint LAL 93-38, July 1993.

[21] H.D. Hildreth, T.L. Barklow and D.L. Burke, Phys. Rev. **D49** (1994) 3441.